ORGANIC MASS SPECTROMETRY, VOL. 28, 1135–1143 (1993)

The Precursor Scan. A New Type of Experiment in Neutralization–Reionization Mass Spectrometry†

Ming Gu and František Tureček
Department of Chemistry, BG-10, University of Washington, Seattle, Washington 98195, USA

A new scan technique utilizing the tandem quadrupole acceleration–deceleration mass spectrometer is described. The technique is based on combined monitoring of neutral and ion precursors that fragment following collisional *electron transfer* to give rise to a selected low-mass neutral species and its ion, respectively. $PO^{\cdot}$ is found to be a stable neutral species formed by dissociations of a variety of oxidized phosphorus compounds, such as di- and trialkyl phosphites, phosphates and phosphonic esters. These compounds can be selectively monitored through $PO^{\cdot}$ precursor scans in multi-component mixtures. Interferences from isobaric neutral species, $^{35}ClC^{\cdot}$, $CH_3S^{\cdot}$, $CH_3\,^{30}SiH_2^{\cdot}$, and their precursors are discussed. *Neutralization–reionization spectra of phosphorus-containing* radicals, $PO^{\cdot}$, $CH_3OPH^{\cdot}$, $CH_3OPOH^{\cdot}$, $^{\cdot}P(OCH_3)_2$ and $(CH_3O)_2PO^{\cdot}$, are also reported.

INTRODUCTION

Tandem mass spectrometry has been used extensively for ion structure studies and mixture analysis.[1,2] A number of scanning techniques have been devised to monitor *unimolecular* dissociations of metastable ions and collisionally activated dissociations (CAD) of stable ions at low (1–100 eV) and high (keV) laboratory energies.[3–8] Especially promising for mixture analysis are those techniques that select the ions of interest and monitor their dissociations with an appropriate functional relationship of the precursor and product ion mass to charge ratios, such as the constant neutral loss[4] and reaction intermediate scans,[7] as summarized by Schwartz and co-workers.[8,9] Precursor ion scans have also been developed to monitor all ions dissociating to give rise to a fragment of a selected mass.[3,5] This can be carried out on a triple quadrupole instrument by scanning the first quadrupole mass analyzer while keeping the third analyzer tuned to an ion of the given m/z, or on a sector instrument by scanning the magnet (B) and electric (E) sectors while maintaining the B^2/E ratio constant, by scanning the accelerating voltage (V), or both V and E while keeping the V/E^2 ratio constant.[1,2] Linked scans on sector instruments are prone to artifacts.[3] Precursor ion scans allow one to screen, *inter alia*, mixtures for the presence of components carrying a given functional group that directs the fragmentation to form a characteristic low-mass ion.[4]

A common feature of these tandem mass spectrometric techniques is their reliance on *ion* chemistry. This brings some disadvantages in that only charged species are observed whereas the complementary neutral fragments are not, and ion dissociations that have high critical energies may not compete on the microsecond time-scale to give rise to observable ion products.[10] By contrast, dissociations of neutral species, as studied by neutralization–reionization mass spectrometry (NRMS),[11,12] have been shown to provide a wealth of information on ion structure and stability, which is often complementary to that provided by CAD of ions. In NRMS, an ion of kiloelectronvolt kinetic energy undergoes electron transfer on collision with a gaseous target, the neutral species is allowed 0.1–5 μs to dissociate and the neutral products are reionized by collisions with another gas, mass analyzed and detected. Following neutralization and reionization, the product ion abundances, relative to that of the precursor ion, depend on the cross-sections for the charge-transfer reactions and on the stabilities of the ions and their corresponding neutral intermediates. For example, ionized atoms and stable small molecules, such as $S^{+\cdot}$,[13,14] $CO^{+\cdot}$,[15,16] $SO^{+\cdot}$,[17,18] $CS^{+\cdot}$,[19] $HCN^{+\cdot}$,[20,21] $C_2H_2^{+\cdot}$ [22,23] and $C_4H_2^{+\cdot}$,[24] are often abundant in the NR mass spectra of cations. Neutral fragments that are indicative of the presence of a functional group, e.g. S and CS for divalent sulfur in thiols, sulfides and ions derived therefrom, can possibly be used as markers for selective screening of these compounds in mixtures.

In this paper we describe a new scan technique utilizing the stability of $PO^{\cdot}$ and its ion PO^+ to monitor organophosphorus compounds in mixtures. Neutral $PO(X\,^2\Pi)$ is a stable radical with a large bond dissociation energy [$D(P—O) = 598\ kJ\ mol^{-1}$] and a relatively low ionization energy ($IE = 8.39$ eV).[25,26] Dissociation of the ion $PO^+(X\,^1\Sigma^+)$ to P^+ and O is even more endothermic [$D(P—O) = 800\ kJ\ mol^{-1}$].[27] These properties should favor the formation of neutral $PO^{\cdot}$ on dissociation of oxidized phosphorus species following neutralization of their ions. PO^+ ions are formed on electron impact ionization of phosphites, phosphates and phosphonates,[28–30] and also by CAD

---

† Dedicated to Professor J. L. Holmes on the occasion of his retirement as Editor of *Organic Mass Spectrometry*.

0030–493X/93/101135–09 $09.50

Received 16 April 1993
Revised manuscript received 21 June 1993
Accepted 23 June 1993

of stable ions derived therefrom,[29–32] and thus appear suitable as a marker for compounds having P—O bonds.

EXPERIMENTAL

The measurements were made on the tandem quadrupole acceleration–deceleration (QADQ) mass spectrometer described recently.[33,34] Briefly, ions formed in the ion source are accelerated to 80–90 eV, transmitted by a quadrupole mass filter floated at 40–50 V as MS-1, accelerated to 8150 eV and neutralized in a collision cell floated at the acceleration voltage. Xenon at a pressure such as to provide 70% transmittance of the ion beam was used in all measurements, unless specified otherwise. The remaining ions are reflected by a cylindrical conduit floated at +250 V, and the fast neutral species are allowed to drift to the reionization cell located 60 cm downbeam and floated at a variable deceleration potential (0 to −8150 V). This corresponds to neutral lifetimes, τ_N (μs) = $0.48\sqrt{m/z}$, of 3.3–6.4 μs for precursor ions of m/z 47–182. The neutral species are reionized to cations by collisions with oxygen at 70% transmittance, the ions formed are decelerated to 80–90 eV, energy filtered in an asymmetric electrostatic lens[33] and mass analyzed by a second quadrupole mass filter as MS-2. The ion lifetime before deceleration is defined by the ion mass and path length,[33] τ_i (μs) = $0.056\sqrt{m/z}$, which is substantially shorter than the neutral lifetime. Observation of neutral dissociations is therefore enhanced. To obtain conventional $^+NR^+$ mass spectra, the deceleration potential is scanned in link with the MS-2 quadrupole to pass ions of preselected combination of mass (m/z) and kinetic energy.

To obtain a precursor spectrum, MS-1 is set to the r.f.-only mode[35] to pass ions of a broad range of m/z produced in the ion source, the MS-2 quadrupole mass filter is set to pass the product ion of mass m_f with unit mass resolution and the deceleration potential is scanned from zero to the nominal value (−8150 V). The product ion of mass m_f, formed by neutral reionization and transmitted at the deceleration potential U_{dec}, must satisfy the equation

$$U_{acc}\frac{m_f}{m_P} - U_{dec} = \Delta U \qquad (1)$$

where m_P is the precursor mass, and U_{acc} is the (constant) acceleration voltage. Product ions formed by neutralization–reionization without dissociation are transmitted at nominal $U_{dec} = U_{acc} - \Delta U$, where ΔU is the kinetic energy loss on charge transfer (15–20 eV),[36,37] while those formed by fragmentation will be transmitted at lower U_{dec} given by Eqn (1). A linear scan of U_{dec} results in a nonlinear mass scale with $U_{dec} + \Delta U \rightarrow 0$ corresponding to $m_P \rightarrow \infty$. The precursor mass resolution ($m_P/\Delta m_P$) decreases with increasing m_P according to the equation

$$\frac{m_P}{\Delta m_P} = -\frac{U_{dec}}{\Delta U_{dec}} = \sqrt{\frac{m_f U_{acc}}{16T(m_P - m_f)}} \qquad (m_P > m_f) \qquad (2)$$

where T is the kinetic energy release in the formation of m_f. This leads to both peak broadening and a compressed mass scale at higher m_P, resulting in less-than-unit precursor-ion mass resolution. Nevertheless, the mass assignment accuracy was within ±0.2 u within the m/z 47–182 scan range for precursors at non-adjacent m/z values. A linked scan of the MS-1 quadrupole mass analyzer and U_{dec}, while keeping their product $m_P U_{dec}$ constant, would improve the precursor mass resolution, but this was not attempted in the present work.

The precursor ion relative abundances depend on the ion transmissions through the MS-1 r.f.-only quadrupole mass filter. The ion transmission is mass dependent and shows periodicity for the given a.c. voltage amplitude and d.c. pole offset, the latter determining the ion laboratory kinetic energy within the quadrupole filter.[38] Similar effects have been reported for ion transmission through r.f.-only quadrupole filters on hybrid instruments.[39] To maintain day-to-day reproducibility of ion relative abundances within ±5%, the parameters affecting the ion transmission (repeller, ion source and quadrupole d.c. voltages and a.c. voltage amplitude) were kept constant. The long-term reproducibility over a period of several months was ±30% owing to different tuning conditions.

The compounds used in this study were purchased from Aldrich and used without further purification. $(CD_3O)_3P$ was synthesized by a standard procedure[40] using CD_3OD, PCl_3 and pyridine. Liquids of b.p. > 150 °C were sampled at 25 °C from a liquid introduction probe directly to the ion source at 3×10^{-6} Torr (corrected) (1 Torr = 133.3 Pa) as measured with a Bayard–Alpert ionization gauge attached to the sidearm on the diffusion pump intake. The sample pressure was regulated with a Teflon needle valve. More volatile liquids were injected into a heated glass reservoir at 100 °C and sampled into the ion source through a variable leak valve. The ion source conditions were: emission current 400 μA and temperature 180 °C. $^+NR^+$ and neutral precursor mass spectra were measured using a PC-based data system,[41] which was modified to provide raw data files in the ASCII code. The reported spectra are averages of 10–25 repetitive scans.

RESULTS AND DISCUSSION

In NRMS, both neutral and ion dissociations can take place depending on the energy deposited in the neutralization and reionization steps, and stabilities of the neutral intermediates and their ion counterparts.[37] Overlapping neutral and ion dissociations are likely to contribute to the formation of the product ion selected as marker species in the precursor scans described above, as depicted by the familial relationship[9] in Scheme 1. The product ion m_f being detected at a fixed m/z value can arise by neutralization–reionization of a

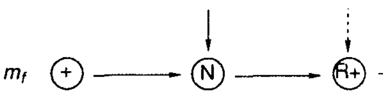

Scheme 1

stable precursor ion of the same mass m_f, reionization of a neutral of mass m_f formed by neutral dissociations (N) of a precursor of mass m_P, or by fragmentation of an ion of m_P following reionization (R +). The latter two processes are inseparable in a precursor scan. Although, in general, neutral and ion dissociations cannot be separated in NRMS, they can be distinguished by deuterium labeling, provided that the dissociation mechanisms for neutral species and ions differ, by kinetic techniques[42] or by simple comparison of CAD and NR spectra. For example, ion fragmentations of trimethyl phosphite (**1**) on electron impact (EI) and CAD have been studied in detail,[29,31] so the corresponding spectra can be used as a reference to assess the contributions from ion dissociations in the NMR spectra of **1** and its fragments. In the following we first discuss the $^+NR^+$ dissociations of common fragment ions that appear in the EI spectra of oxidized phosphorus compounds.

Neutralization–reionization of oxidized phosphorus ions

The $^+NR^+$ spectrum of PO^+ produced by EI of **1** [Fig. 1(a)] shows an abundant survivor ion at *m/z* 47 (60% of the total reionized current, %Σ[NR]), and a relatively high NR efficiency[43] of 0.46% [Fig. 1(a)]. The presence of small peaks at *m/z* 14 and 15 indicates an isobaric admixture, possibly CH_4P^+. Indeed, the EI mass spectrum of tri[D_3]methyl phosphite (**2**) displays ions at *m/z* 47 (major) and 51 due to the presence of PO^+ and CD_4P^+, respectively. The $^+NR^+$ spectrum of PO^+ prepared from **2** shows no peaks at *m/z* 14 and 15. A small (~0.5%) peak of doubly charged $PO^{2+\bullet}$ appears at *m/z* 23.5 in the $^+NR^+$ spectra of $\mathbf{1}^{+\bullet}$ and $\mathbf{2}^{+\bullet}$.

The $^+NR^+$ spectra of other ions produced by EI of **1**, e.g. CH_3OPH^+ at *m/z* 63 [Fig. 1(b)], CH_3OP^+OH at *m/z* 79 [Fig. 2(a)], $CH_3OP^+OCH_3$ at *m/z* 93 [Fig. 2(b)], $CH_3OP^+(O)OCH_3$ at *m/z* 109 [Fig. 2(c)], and $\mathbf{1}^{+\bullet}$ [Fig. 3(a)] all show abundant PO^+ products at *m/z* 47. The stability of the corresponding radicals formed by Xe neutralization decreases with the increasing ion mass, and becomes negligible for $CH_3OP(O^\bullet)OCH_3$ [Fig. 2(c)]. Dissociations of **1** following neutralization are qualitatively similar to those observed on electron impact (EI) and CAD,[29,31] with the exception of the CH_2O elimination, which is negligible in $^+NR^+$. However, Fig. 2 shows that, in general, neutralization and reionization results in much deeper dissociation than observed on CAD of the corresponding ions.[29–31]

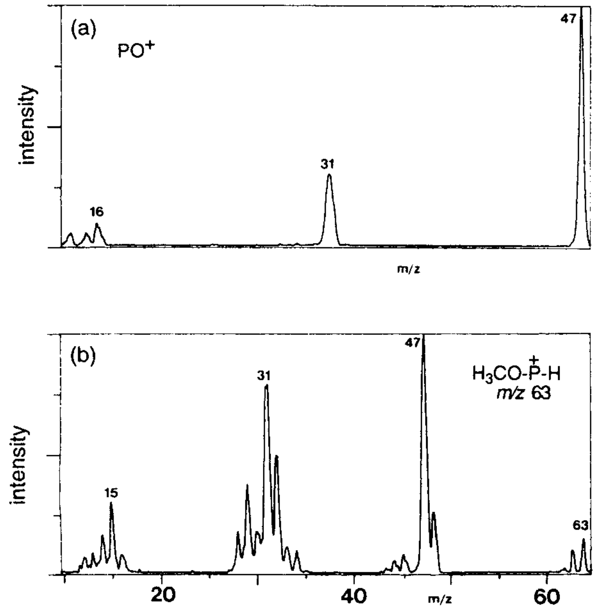

Figure 1. $^+NR^+$ mass spectra obtained with Xe at 70% transmittance (*T*) and oxygen at 70% *T* of (a) PO^+, *m/z* 47, and (b) CH_3OPH^+, *m/z* 63, from **1**. The NR efficiencies, relative to the incident precursor ion abundance, were $\Sigma[NR]/[PO^+] = 0.0046$ and $\Sigma[NR]/[CH_3OPH^+] = 0.0042$.

Further, the $^+NR^+$ spectra of the deuterium-labeled derivative $\mathbf{2}^{+\bullet}$ and its fragment ions reveal neutral dissociations that differ qualitatively from those of ions observed in the EI mass spectrum (Table 1). For example, whereas losses of $CD_3^\bullet$ and $CD_3O^\bullet$ are observed in both $^+NR^+$ and EI of **2** (*m/z* 115 and 99, respectively), the consecutive loss of $CD_3O^\bullet$ from the $(M - CD_3)$ fragment occurs only in $^+NR^+$ (*m/z* 81). This is in line with the even-electron rule,[10,44] according to which formation of odd-electron species is disfavored in even-electron ion dissociations. No such restriction applies to neutral dissociations in which formation of the stable $CD_3OP{=}O$ molecule from the radical pre-

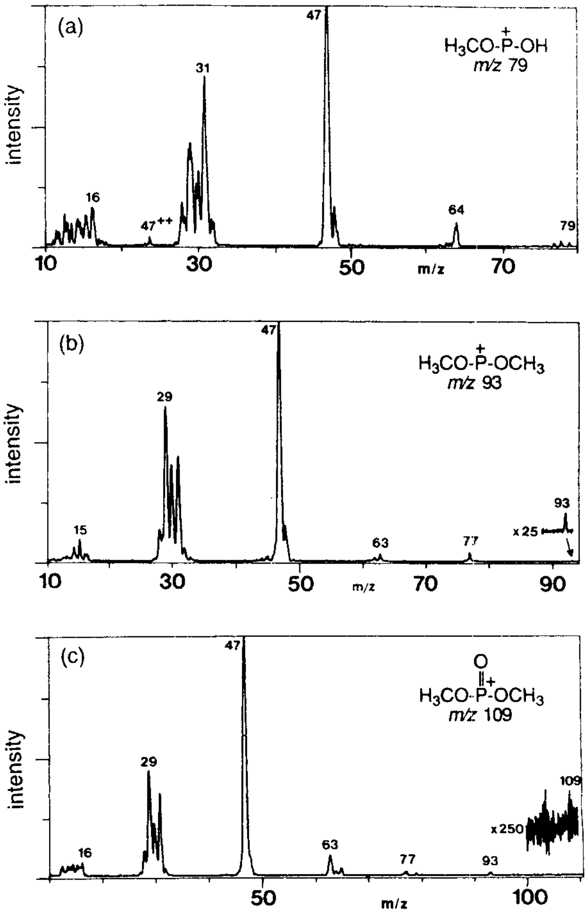

Figure 2. $^+NR^+$ mass spectra of (a) CH_3OP^+OH, *m/z* 79, (b) $CH_3OP^+OCH_3$, *m/z* 93, and (c) $CH_3OP^+(O)OCH_3$, *m/z* 109, from **1**. The NR efficiencies were $\Sigma[NR]/[m/z\ 79] = 0.0021$, $\Sigma[NR]/[m/z\ 93] = 0.0012$ and $\Sigma[NR]/[m/z\ 109] = 0.0020$.

Table 1. $^{+}NR^{+}$ **spectra (Xe, 70%** T/O_2**, 70%** T**) of** $(CD_3O)_3P^{+\cdot}$ **(**$2^{+\cdot}$**) and its fragment ions**

	Relative intensity (%)					
m/z	$2^{+\cdot}$	$(CD_3O)_2P^{+}{=}O$	$(CD_3O)_2PD^{+\cdot}$	$(CD_3O)_2P^{+}$	$CD_3OP^{+}OD$	CD_3OPD^{+}
133	<0.02					
115	4.1	0.1				
101	1	—	0.2			
99	10.6	—	4.5	0.6		
95	2.3	1.2	—	—		
83	3.5	—	1.4	—	0.5	
81	3.7	1.3	0.6	—	0.4	
79	6.3	3.1	0.5	2.8	2.2	
67	1.5	1.8	1.7	—	0.4	13
65	4.9	4.2	3.3	1.1	7.0	4.8
63	8.2	9.2	2.2	2.0	2.8	0.8
53	—	—	—	—	1.2	
51	1.2	—	—	0.8	2	
49	12.7	5.2	5.6	18.3	16.9	21.7
47	100	100	98.6	100	100	100
37	—	—	—	—	—	4.9
36	—	—	—	—	2.8	—
35	—	—	1.4	—	—	10.6
34	8.5	4.3	10.6	7	11.3	—
33	2.1	1.2	4.3	2	1.5	33.8
32	19.7	15.5	50	25.6	18.7	15.5
31	9.8	12.0	39.5	24.6	22.5	55.6
30	49.3	26.1	100	50.7	21.8	29.6
28	5.6	4.8	20.1	4.9	7.7	11.3
18	7.0	2.4	12.7	2.8	4.2	10.8
16	19	4.2	15.5	2.5	14.8	14.1
14	12.7	1.5	4.4	0.7	7	1.5
12	2.1	1.0	1	0.3	4	0.4

cursor is favored. Reionization of the $CD_3O^{\cdot}$ neutral species gives a fragmentation pattern typical of the methoxy structure,[45] $[CO^{+\cdot}]:[CDO^{+}]:[CD_2O^{+\cdot}]:[CD_3O^{+}] = 20:100:50:10$, indicating a direct P—O bond cleavage in the neutral precursor. This is analogeous to $CH_3O^{\cdot}$ formation from trimethyl borate,[43] but contrasts with CH_3O loss from methyl acetate, which yields mixtures of $CH_3O^{\cdot}$ and $^{\cdot}CH_2OH$ isomers.[43,45] Very abundant $CD_3O^{\cdot}$ formation is observed in the $^{+}NR^{+}$ spectrum of the $(M - CD_2O)^{+\cdot}$ ion, m/z 101, formed from $2^{+\cdot}$ by rearrangement. Since no methanol elimination from m/z 101 is observed on NR, the ion is likely to have the phosphine structure, $(CD_3O)_2PD^{+\cdot}$, rather than that of a distonic isomer, $CD_3O{—}P^{\cdot}{—}O^{+}(D)CD_3$. On neutralization the latter would form a hypervalent–hypovalent biradical that could be expected readily to eliminate methanol, in contrast to what is observed in the spectrum (Table 1).

The fragment at m/z 63 shows the expected mass shift to m/z 67 in the EI mass spectrum of **2**, consistent with the CD_3OPD^{+} structure. By contrast, a fragment at m/z 63 is found in the $^{+}NR^{+}$ spectra of most deuterium-labeled precursor ions (Table 1), indicating $PO_2^{\cdot}$ as the neutral dissociation product. Neutral $CD_3OP^{\cdot}OD$ (from m/z 83, Table 1) loses $CD_3^{\cdot}$ and/or $OD^{\cdot}$ radicals to give PO_2D and/or CD_3OP, whereas the elimination of CD_4 and/or D_2O molecules is less abundant. The NR spectrum of CD_3OPD^{+} (m/z 67) is compatible with the assumed structure, showing $CD_3^{\cdot}$, $CD_3O^{\cdot}$ and a series of PD_x fragments at m/z 37, 35, 33 and 31, but no CD_3OD (Table 1).

Fragmentations of neutral **1** and **2** indicate that the corresponding stable ions $1^{+\cdot}$ and $2^{+\cdot}$ do not isomerize to the distonic forms that would form ylids or biradicals on neutralization. This is especially corroborated by the absence of peaks for the loss of CH_2O, CH_3OH and their isotopomers in the NR spectra of **1** [Fig. 3(b)] and **2** (Table 1), respectively. The elimination of CH_2O from unstable $1^{+\cdot}$, as observed in the EI mass spectrum, may involve a distonic intermediate, and can be rationalized by the formation of a classical dimethoxyphosphine structure as discussed above. The dominant formation of PO involves multiple P—O and C—O bond cleavages which are likely to occur in consecutive dissociations. Note that neutral $PO^{\cdot}$ is *not* lost on CAD of oxidized phosphorus ions,[29–32] although the CAD spectra do show PO^{+} ions of moderate relative abundances that increase with increasing collision energy.[31] Since most of the neutral precursors dissociate prior to reionization, only a small fraction of PO^{+} found in the $^{+}NR^{+}$ spectra can be due to ion dissociations following reionization, while the major fraction must be due to neutral unimolecular dissociations. Note that ion dissociations induced by collisions with the neutralization gas cannot be a major source of $PO^{\cdot}$, as its loss is not observed in the CAD spectra of ions from **1**. Also, neutral dissociations should be slightly preferred on the basis of the longer neutral residence times, e.g. 5.3 μs for unimolecular dissociations of the neutral species following ion neutralization, as opposed to 0.2 μs for CAD of the m/z 124 ion in the neutralization cell and 0.6 μs for CAD of the same ion following reionization.

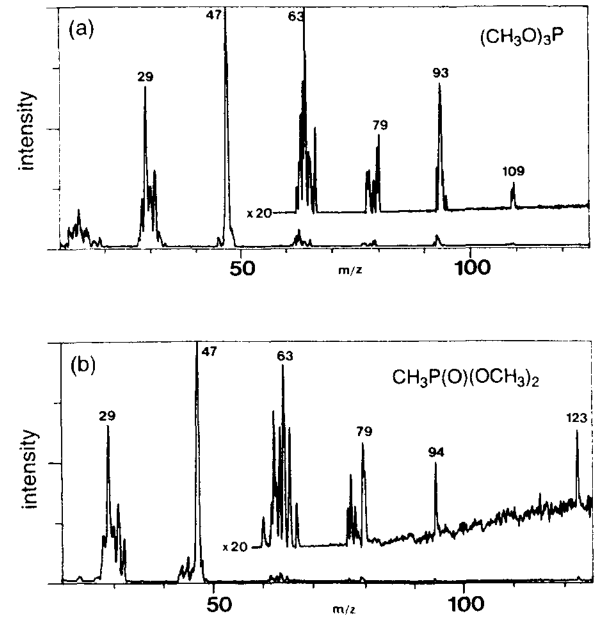

Figure 3. $^+$NR$^+$ mass spectra of (a) **1** and (b) **3**. The NR efficiencies were $\Sigma[\mathrm{NR}]/[\mathbf{1}^{+\bullet}] = 0.0016$ and $\Sigma[\mathrm{NR}]/[\mathbf{3}^{+\bullet}] = 0.00061$.

The $^+$NR$^+$ mass spectrum of dimethyl methylphosphonate (**3**) is distinctly different from that of **1**. Figure 3(b) shows that the survivor ion is absent, as is the $(\mathrm{M}-\mathrm{CH_3})^+$ fragment at *m/z* 109 and $(\mathrm{M}-\mathrm{CH_3O})^+$ at *m/z* 93.[29] The loss of H$^\bullet$ and CH_2O from **3** is compatible with the formation of a biradical intermediate by neutralization of a distonic ion which in turn was formed by hydrogen rearrangement in the molecular ion, as suggested previously in a CAD study.[29] Similar to that of **1**, the $^+$NR$^+$ spectrum of **3** is dominated by the PO$^+$ peak at *m/z* 47.

Scans of neutral PO$^\bullet$ precursors

The facile formation on neutralization–reionization of PO$^+$ from $\mathbf{1}^{+\bullet}$, $\mathbf{3}^{+\bullet}$ and their dissociation products is corroborated by the corresponding PO precursor scans. That of **1** shows all the important precursor ions at *m/z* 124, 109, 93, 79 and 63 [Fig. 4(a)], and represents a fingerprint of neutral and, to a lesser extent, ion dissociations corresponding to the precursor ion relative abundances in the EI mass spectrum of **1**. The conversion efficiency to PO$^+$, defined as the sum of precursor peak areas relative to that of the incident PO$^+$, Σ[NR]/[*m/z* 47], was 0.0025 for **1**. The different relative intensities of the peaks in the EI mass spectrum compared with those in the precursor scan result from different neutralization efficiencies of the ion species, and different yields of PO$^\bullet$ from the corresponding neutral species and PO$^+$ from ions after reionization (Figs 1 and 2). The different PO$^\bullet$ yields from ions at *m/z* 109 and 79 in the precursor spectra of **1** and **3** suggest distinct structures for these ions. Also, the molecular ions $\mathbf{1}^{+\bullet}$ and $\mathbf{3}^{+\bullet}$ show very different PO$^\bullet$ yields [Fig. 3(a) and (b)]. The very small peak of the *m/z* 124 precursor from $\mathbf{3}^{+\bullet}$ [Fig. 4(d)] is surprising in view of the dominant formation of PO$^\bullet$ in the $^+$NR$^+$ mass spectrum; however, the $^+$NR$^+$ efficiency of $\mathbf{3}^{+\bullet}$ is significantly lower than that of $\mathbf{1}^{+\bullet}$ (Fig. 3), which may account for the effects observed in the precursor spectra.

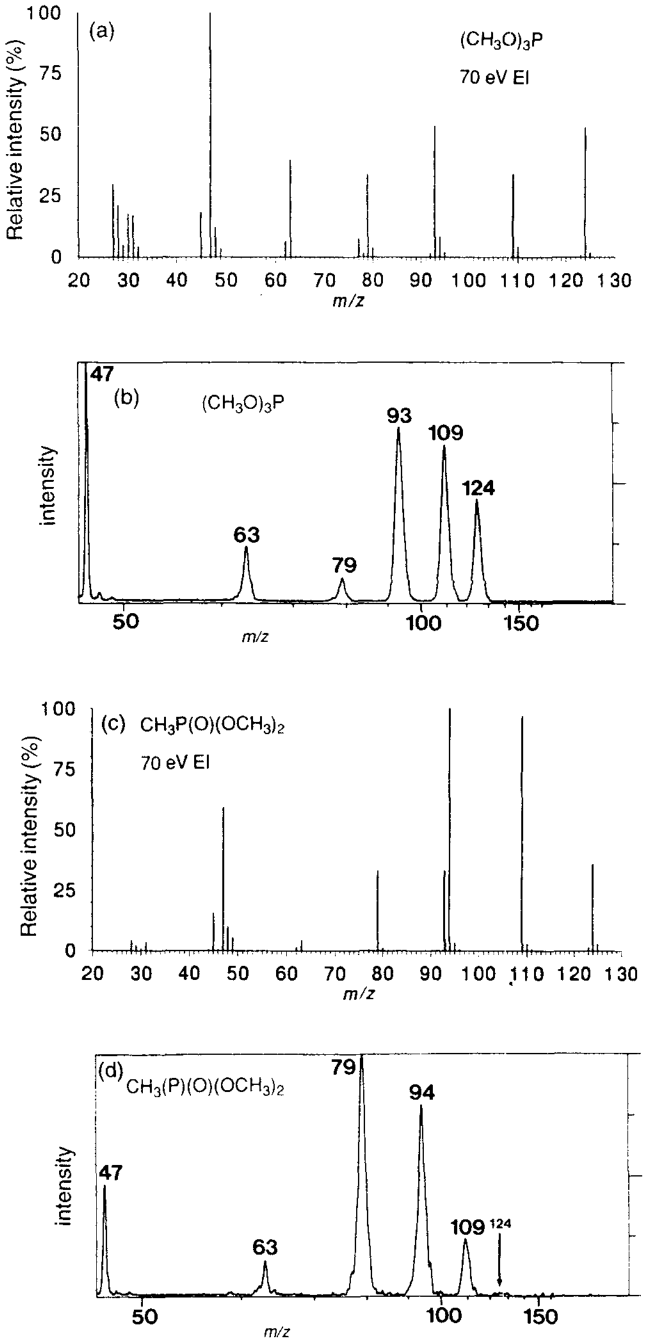

Figure 4. 70 eV EI mass spectra and PO$^\bullet$ precursor scans of (a, b) **1** (Xe/O_2, 70% *T*) and (c, d) **3** (Xe/O_2, 70% *T*).

The precursor peak patterns depend strongly on the neutralization gas, which affects the $^+$NR$^+$ mass spectra of the individual ions and hence also the PO$^\bullet$ yields. For example, neutralization with the softer CH_3SSCH_3 ($IE_a = 7.4$ eV, $IE_v = 8.96$ eV) of ions formed from **1** results in the dominant peak of PO$^+$ at *m/z* 47 (52% Σ[NR]) owing to the charge-exchange reaction, $\mathrm{PO}^+ \rightarrow \mathrm{PO}^\bullet \rightarrow \mathrm{PO}^+$, whereas dissociative PO$^\bullet$ formation is much less abundant, showing 2, 4, 13, 4, 20, 2 and 3% Σ[NR] for precursors at *m/z* 124, 109, 93, 79, 63, 49 and 48, respectively. By contrast, neutralization with the hard helium (IE = 24.6 eV) results in the dominant formation of PO$^\bullet$ by dissociative processes, yielding 14, 38, 33, 5 and 11% Σ[NR] for m/z 124, 109, 93, 79 and 63 precursors, respectively, whereas the peak at m/z 47 from simple charge exchange is negligibly small (0.4% Σ[NR]). This is consistent with the low efficiency of He as an electron donor in collisional neutralization.[46,47] The strong dependence of PO$^\bullet$ yields on the neutralization conditions further points to the dominant role of neutral dissociations in PO$^\bullet$ formation.

The PO$^\bullet$ precursor scans of ions formed from dimethyl phosphite [**4**, Fig. 5(b)], triethyl phosphite [**5**, Fig. 6(b)], triethyl phosphate [**6**, Fig. 7(b)] and trimethyl phosphate [**7**, Fig. 8(b)] show characteristic patterns of precursor ions. These scans seems to emphasize higher mass precursors, as indicated by the increased relative intensities of the m/z 127, 137 and 155 peaks in the precursor scan of **6** compared with those of the corresponding ion peaks in the EI mass spectrum (Fig. 7). Note that the formation of PO$^\bullet$ from **4**–**7** are mostly due to multi-step dissociations. Since most of the precursors are even-electron ions that form radicals on neutralization, e.g. $(C_2H_5O)_2P^+{=}O \rightarrow (C_2H_5O)_2P{-}O^\bullet$ for m/z 137 from **6**, the mechanisms of the ion and neutral dissociations must be different, with the former preferring rearrangements and the latter simple bond cleavages.[10]

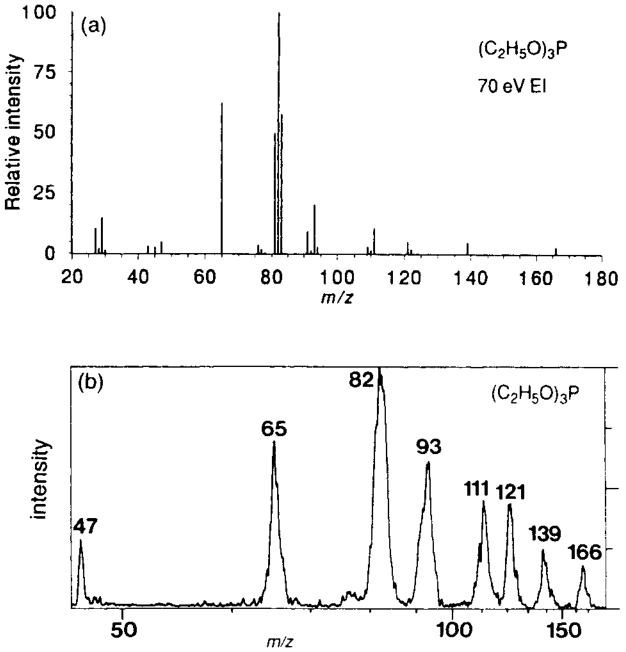

Figure 6. (a) 70 eV EI mass spectrum of triethyl phosphite (**5**) and (b) PO$^\bullet$ neutral precursor scan.

Mixture analysis and interferences

The stability of PO$^\bullet$ and its characteristic precursor patterns have further been utilized to distinguish oxidized phosphorus compounds in mixtures. This was investigated with an artificial mixture of **7** with compounds of various types but comparable volatilities, e.g. 1,6-dichlorohexane, methyl benzoate, nonan-2-one, nonan-3-one, nonan-5-one, 1-aminononane, acetophenone and benzylamine (all components in equal amounts by volume). The EI mass spectrum of the above mixture shows multiple peak overlaps at m/z 65, 79 and 109 obscuring the presence of **7**; the relative abundances of ions from **7** do not exceed 5% [Fig. 8(b)]. By contrast, there is little or no isobaric overlap at m/z 47, so the neutral precursor scan displays only the PO$^\bullet$ precursors corresponding to dissociations of **7** [Fig. 8(c)]. The spectra in Fig 8(a) and (c) were taken on different days,

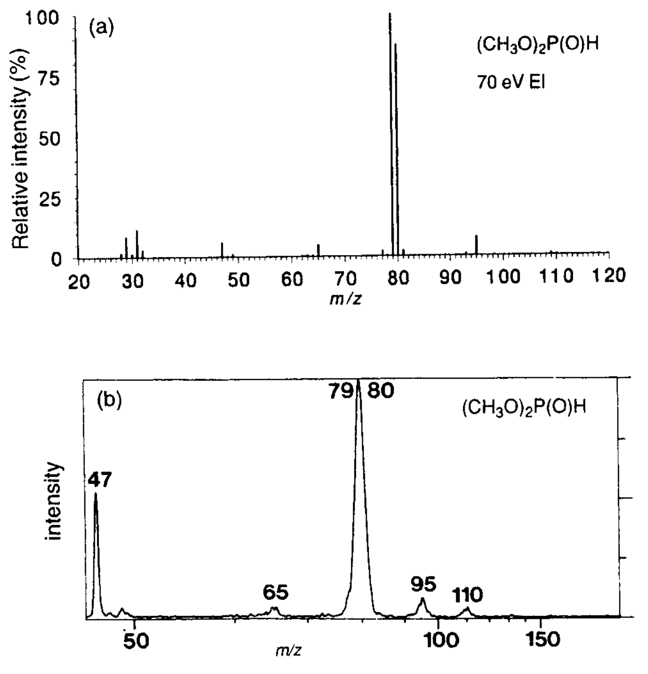

Figure 5. (a) 70 eV EI mass spectrum of dimethyl phosphite (**4**) and (b) PO$^\bullet$ neutral precursor scan.

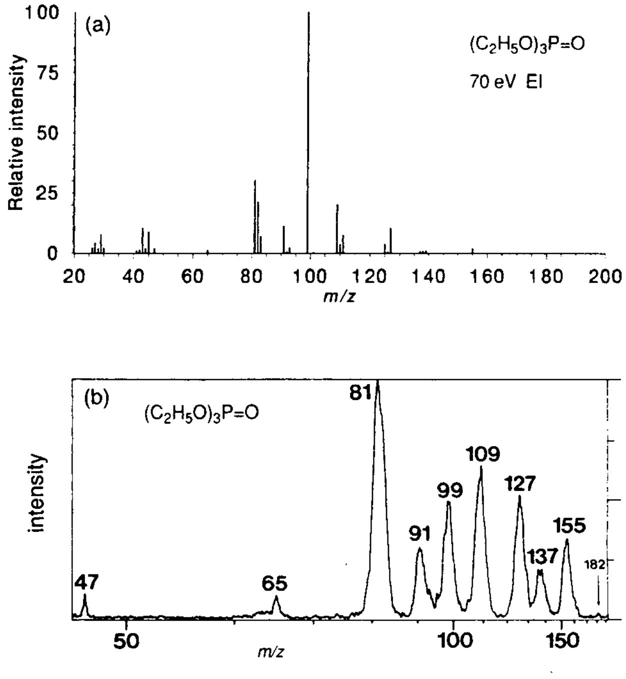

Figure 7. (a) 70 eV EI mass spectrum of triethyl phosphate (**6**) and (b) PO$^\bullet$ neutral precursor scan.

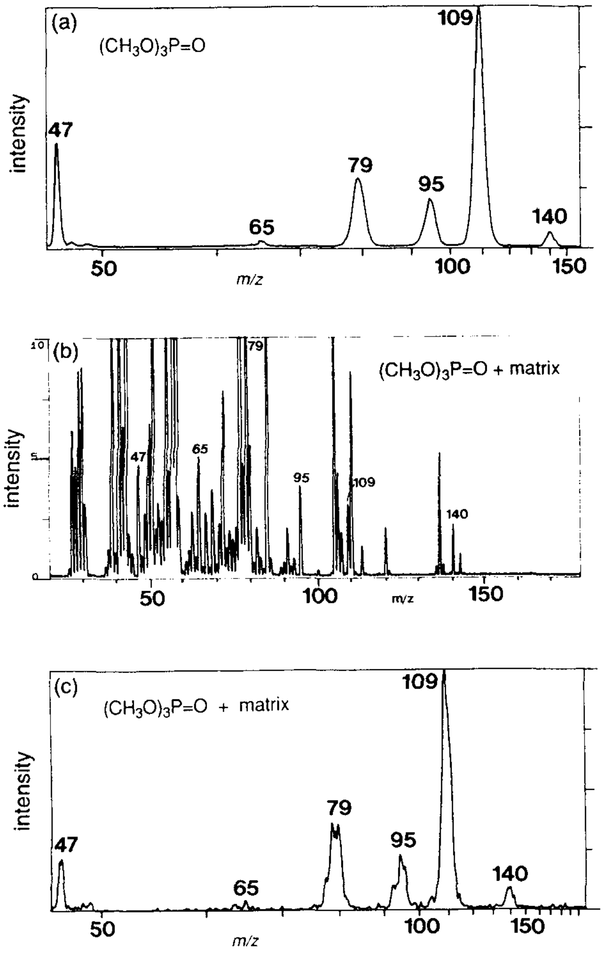

Figure 8. (a) PO$^\bullet$ neutral precursor scan from trimethyl phosphate (**7**), (b) 70 eV EI spectrum of a mixture (the relative intensity scale is expanded 10×) and (c) PO$^\bullet$ neutral precursor scan of **7** in the mixture.

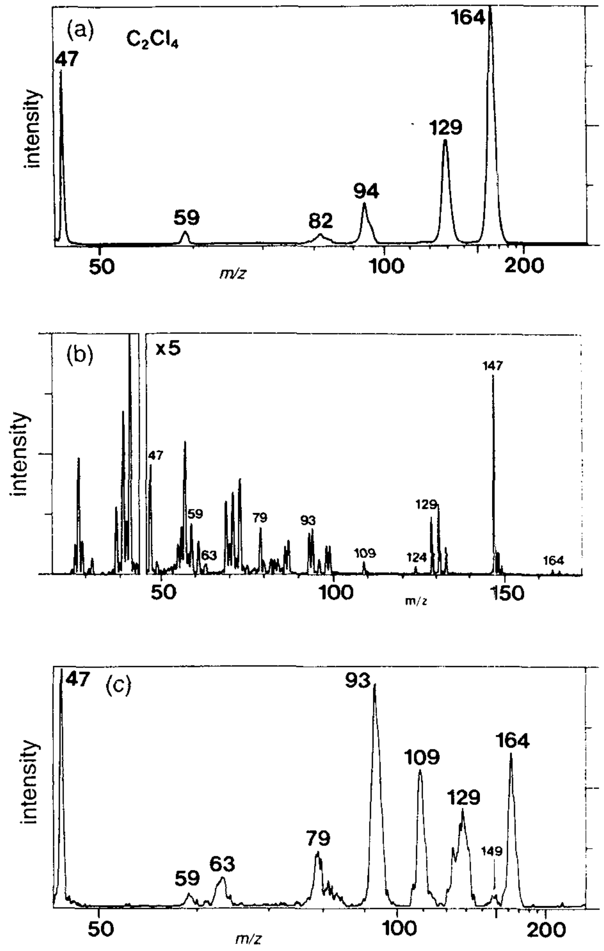

Figure 9. (a) ^{35}ClC$^\bullet$ neutral precursor scan from C_2Cl_4, (b) 70 eV EI mass spectrum and (c) neutral precursor scan of *m/z* 47 from the mixture of **1**, C_2Cl_4 and the matrix.

so there is some variability in the precursor relative intensities, measured as peak areas, as quantified by the correlation coefficient, $s^2 = 0.974$.

Isobaric overlaps of PO$^+$ with $(CH_3)_2OH^+$ and $C_2H_7O^+$ in the EI mass spectra of mixtures do not result in interferences in the neutral precursor spectrum. This is due to the instability of the $(CH_3)_2OH^\bullet$ and $C_2H_7O^\bullet$ radicals, which do not give rise to detectable peaks in the $^+NR^+$ and neutral precursor spectra.[48,49]

Interferences from isobaric overlaps of ions at *m/z* 47 that do form stable neutral species were investigated with **1**, tetrachloroethylene (forming $^{35}ClC^+$) and dimethyl disulfide (forming CH_2SH^+). A mixture of eight compounds with volatilities comparable to that of **1**, i.e. methyl cyclopropanecarboxylate, 2-butyl acetate, 1-propyl acetate, pentan-3-one, 2,4-dimethylpentan-3-one, 1-methylpiperidine, diallyl ether and hexamethyldisiloxane in equal amounts by volume, was used as a matrix. The neutral precursor scan of *m/z* 47 (^{35}ClC) from tetrachloroethylene shows an abundant peak of $^{35}ClC^+$ from charge exchange, $ClC^+ \rightarrow ClC^\bullet \rightarrow ClC^+$, and the peaks of precursors, C_2Cl_4 (*m/z* 164), C_2Cl_3 (*m/z* 129), C_2Cl_2 (*m/z* 94), CCl_2 (*m/z* 82) and C_2Cl (*m/z* 59) [Fig. 9(a)]. Precursors peaks corresponding to different ^{35}Cl and ^{37}Cl isotope combinations are unresolved in these scans. ClC$^\bullet$ is formed very efficiently from C_2Cl_4 and its fragments, giving $\Sigma[NR]/[m/z\ 47] = 0.0105$. In line with the precursor scan the $^+NR^+$ mass spectrum of ClC^+ (Xe/O_2, 70% transmittance) shows an abundant survivor ion, $[ClC^+] = 55\%$ $\Sigma[NR]$, and a moderate NR efficency, $\Sigma[NR]/[ClC^+]_{incident} = 0.0018$. Consequently, the neutral precursor scans of mixtures of **1**, with C_2Cl_4 and the eight-component matrix are composed of peaks originating from both Cl$^-$ and P-containing precursors [Fig. 9(b, c)]. Analysis of precursor scans obtained with 1 : 1, 2 : 1 and 3 : 1 (v/v) mixtures of C_2Cl_4 with **1** showed a linear dependence of the PO$^\bullet$ precursor peak relative intensities on the **1** content (slope 1.01, intercept −0.001). This was further checked by digitially subtracting the ^{35}CCl precursor spectrum from those of the mixtures and comparing the results with the standard spectrum of PO$^\bullet$ from **1** (the data files were translated into the ASCII code and treated with the PROMATLAB program[50]). The correlation coefficients obtained ($s^2 = 0.97$–0.99) were comparable to those for spectra of pure **1** measured on different days.

$^\bullet CH_2SH$, *m/z* 47, is also formed efficiently on Xe neutralization of sulfide precursors, e.g. $\Sigma[NR]/[m/z\ 47] = 0.0016$ from dimethyl disulfide. The neutral precursor scan of the latter shows a dominant peak due to $CH_3SSCH_3^{+\bullet}$, *m/z* 94 (84% Σ[NR]), and smaller peaks

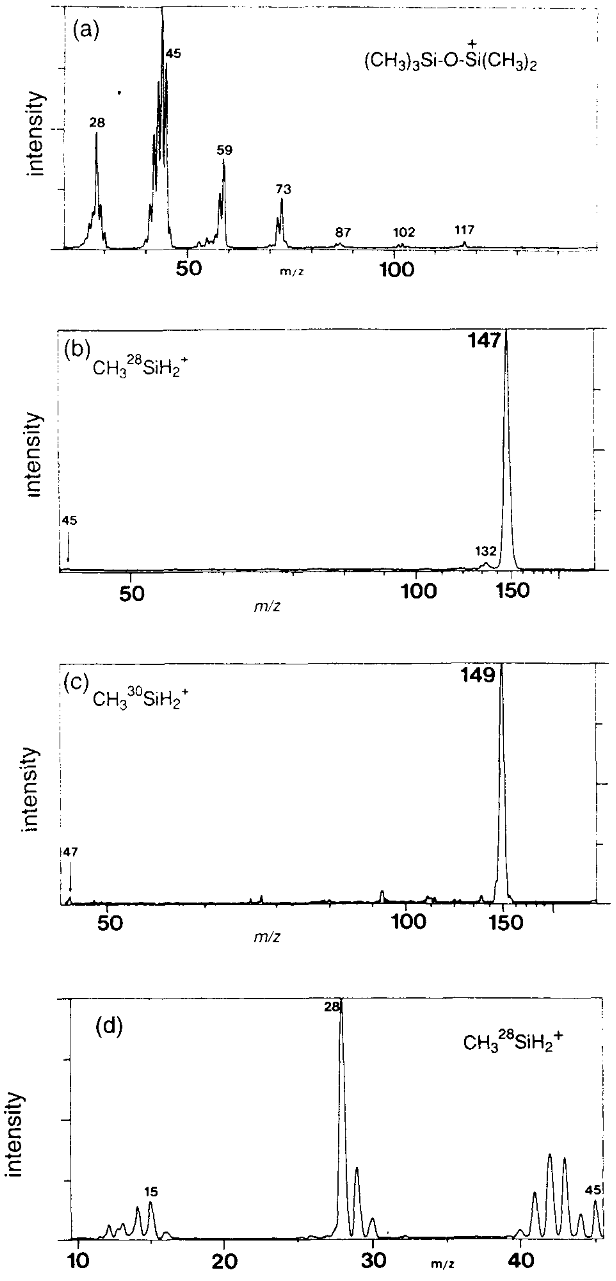

Figure 10. (a) $^+NR^+$ spectrum (Xe, 70% T/O_2, 70% T) of $(CH_3)_3SiOSi^+(CH_3)_2$, (b) neutral precursor scan of m/z 45 from hexamethyldisiloxane, (c) neutral precursor scan of m/z 47 and (d) $^+NR^+$ spectrum of $CH_3{}^{28}SiH_2{}^+$.

due to CH_3SS^+, m/z 79 (5%), $CH_3SH^{+\bullet}$, m/z 48 (5%) and reionized CH_2SH^+ (5%). Digital subtraction of the CH_2SH neutral precursor scan from those of **1**–dimethyl disulfide mixtures also allowed reconstruction of the spectrum of **1**.

Of interest also was the small peak in the precursor scan of the matrix-containing mixture corresponding to a precursor at m/z 149 that does not belong to **1** or C_2Cl_4 [Fig. 9(c)]. The m/z 149 precursor peak was found to originate from the ^{30}Si satellite of the abundant $(CH_3)SiOSi^+(CH_3)_2$ ion from hexamethyldisiloxane, as confirmed by the $^+NR^+$ spectrum of the (^{28}Si, ^{12}C) isotopomer at m/z 147 [Fig. 10(a)], which shows a prominent fragment at m/z 45. Consistent with the NR spectrum, neutral precursor scans of m/z 45 and 47 in the spectrum of pure hexamethyldisiloxane show m/z 147 and 149, respectively, as the predominant precursors [Fig. 10(b) and (c)]. Surprisingly, the $^+NR^+$ spectrum of m/z 45 points to $CH_3SiH_2{}^+$, not $SiOH^+$, as indicated by the consecutive losses of five hydrogen atoms, the presence of SiH_2, CH_4 and CH_3 fragments and the absence of OH [Fig. 10(d)]. Consistent with this finding, the EI mass spectrum of $(CD_3)_3SiOSi(CD_3)_3$ shows a clean shift of m/z 45 to 50. It should be noted that the $CH_3{}^{30}SiH_2{}^+$ ion at m/z 47 is formed from its m/z 149 precursor in a very low yield, $\Sigma[NR]/[m/z\ 47] = 0.00020$, and thus does not represent a serious interference in the $PO^\bullet$ neutral precursor scans.

In conclusion, neutral precursor scans represent a new approach to the monitoring of oxidized phosphorus compounds, based on dissociations that result in the formation of neutral $PO^\bullet$. Common organic compounds such as hydrocarbons, alkyl chlorides, ketones, esters, ethers and amines do not interfere in these measurements. Interferences from polychlorinated hydrocarbons and sulfides can be deconvoluted for known contaminants.

Acknowledgements

Support of this work by the National Science Foundation (grant CHEM 9102442) is gratefully acknowledged. Acknowledgement is also made to the donors of the Petroleum Research Fund of the American Chemical Society for partial support.

REFERENCES

1. F. W. McLafferty (Ed.), *Tandem Mass Spectrometry*. Wiley, New York (1983).
2. K. L. Busch, G. L. Glish and S. A. McLuckey, *Mass Spectrometry/Mass Spectrometry*. VCH, New York (1988).
3. R. P. Morgan, C. J. Porter and J. H. Beynon, *Org. Mass Spectrom.* **12**, 735 (1977).
4. W. F. Haddon, *Org. Mass Spectrom.* **15**, 539 (1980).
5. G. L. Glish and S. A. McLuckey, *Org. Mass Spectrom.* **24**, 470 (1989).
6. M. Vincenti, J. C. Schwartz, R. G. Cooks, A. P. Wade and C. G. Enke, *Org. Mass Spectrom.* **23**, 579 (1988).
7. J. R. O'Lear, L. G. Wright, J. N. Louris and R. G. Cooks, *Org. Mass Spectrom.* **22**, 348 (1987).
8. J. C Schwartz, K. L. Schey and R. G. Cooks, *Int. J. Mass Spectrom. Ion Processes* **101**, 1 (1990).
9. J. C. Schwartz, A. P. Wade, C. G. Enke and R. G. Cooks, *Anal. Chem.* **62**, 1809 (1990).
10. F. W. McLafferty and F. Turecek, *Interpretation of Mass Spectra*, 4th edn. University Science Books, Mill Valley, CA (1993).
11. P. O. Danis, C. Wesdemiotis and F. W. McLafferty, *J. Am. Chem. Soc.* **105**, 7454 (1983).
12. P. C. Burgers, J. L. Holmes, A. A. Mommers and J. K. Terlouw, *Chem. Phys. Lett.* **102**, 1 (1983).
13. M. Gu and F. Turecek, *J. Am. Chem. Soc.* **114**, 7146 (1992).
14. A. Masquestiau, R. Flammang, M. Plisnier, C. Wentrup, P. Kambouris, M. R. Paton and J. K. Terlouw, *Int. J. Mass Spectrom. Ion Processes* **100**, 477 (1990).
15. F. Turecek, D. E. Drinkwater and F. W. McLafferty, *J. Am. Chem. Soc.* **113**, 5950 (1991).

16. D. Sulzle, P. E. O'Bannon and H. Schwarz, *Chem. Ber.* **125**, 279 (1992).
17. F. Turecek, D. E. Drinkwater and F. W. McLafferty, *J. Am. Chem. Soc.* **111**, 7696 (1989).
18. F. Turecek, F. W. McLafferty, B. J. Smith and L. Radom, *Int. J. Mass Spectrom. Ion Processes* **101**, 283 (1990).
19. D. Sulzle and H. Schwarz, *Angew. Chem., Int. Ed. Engl.* **27**, 1337 (1988).
20. T. Wong, J. Warkentin and J. K. Terlouw, *Int. J. Mass Spectrom. Ion Processes* **115**, 33 (1992).
21. R. Flammang, O. Thoelen, C. Quattrocchi and J.-L. Bredas, *Rapid. Commun. Mass Spectrom.* **6**, 135 (1992).
22. R. E. March and A. B. Young, *Int. J. Mass Spectrom. Ion Processes* **76**, 11 (1987).
23. F. Turecek and M. Gu, *Org. Mass Spectrom.* **27**, 1335 (1992).
24. M.-Y. Zhang, B. K. Carpenter and F. W. McLafferty, *J. Am. Chem. Soc.* **113**, 9499 (1991).
25. J. M. Dyke, A. Morris and A. Ridha, *J. Chem. Soc., Faraday Trans. 2* **78**, 2077 (1982).
26. P. F. Zittel and W. C. Lineberger, *J. Chem. Phys.* **65**, 1236 (1976).
27. S. G. Lias, J. E. Bartmess, J. F. Liebman, J. L. Holmes, R. D. Levin and G. W. Mallard, *J. Phys. Chem. Ref. Data* **17**, Suppl. 1 (1988).
28. F. W. McLafferty and D. B. Stauffer, *The Wiley/NBS Registry of Mass Spectral Data*. Wiley, New York (1989).
29. J. R. Holtzclaw, J. R. Wyatt and J. E. Campana, *Org. Mass Spectrom.* **20**, 90 (1985).
30. J.R. Holtzclaw and J. R. Wyatt, *Org. Mass Spectrom.* **23**, 261 (1988).
31. L. Zeller, J. Farrell, Jr, P. Vainiotalo and H. I. Kenttamaa, *J. Am. Chem. Soc.* **1114**, 1205 (1992).
32. L. C. Zeller, J. T. Farrell, Jr, H. I. Kenttamaa and T. Kuivalainen, *J. Am. Soc. Mass Spectrom.* **4**, 125 (1993).
33. F. Turecek, M. Gu and S. A. Shaffer, *J. Am. Soc. Mass Spectrom.* **3**, 493 (1992).
34. F. Turecek, *Org. Mass Spectrom.* **27**, 1087 (1992).
35. P. H. Dawson, *Mass Spectrom. Rev.* **5**, 1 (1986).
36. J. Bordas-Nagy, J. L. Holmes and C. E. C. A. Hop, *Int. J. Mass Spectrom. Ion Processes* **94**, 189 (1989).
37. J. L. Holmes, *Mass Spectrom. Rev.* **8**, 513 (1989).
38. P. H. Dawson and J. E. Fulford, *Int. J. Mass Spectrom. Ion Phys.* **42**, 195 (1982).
39. A. J. Alexander and R. K. Boyd, *Int. J. Mass Spectrom. Ion Processes* **90**, 211 (1989).
40. K. Sasse, in *Methoden der Organische Chemie* (*Houben-Weyl*), ed. by E. Muller, O. Bayer, H. Meerwein and K. Ziegler, Vol. XII/2, p. 55, Georg Thieme, Stuttgart (1964).
41. D. E. Drinkwater, F. Turecek and F. W. McLafferty, *Org. Mass Spectrom.* **26**, 559 (1991).
42. D. W. Kuhns and F. Turecek, paper presented at the 41st ASMS Conference on Mass Spectrometry and Applied Topics, San Francisco, 1993, communication No. ThP103.
43. C. Wesdemiotis, R. Feng, E. R. Williams and F. W. McLafferty, *Org. Mass Spectrom.* **21**, 689 (1986).
44. M. Karni and A. Mandelbaum, *Org. Mass Spectrom.* **15**, 53 (1980).
45. J. K. Terlouw, J. L. Holmes and P. C. Burgers, *Int. J. Mass Spectrom. Ion Processes* **66**, 239 (1985).
46. P. O. Danis, R. Feng and F. W. McLafferty, *Anal. Chem.* **58**, 348 (1986).
47. C. E. C. A. Hop and J. L. Holmes, *Org. Mass Spectrom.* **26**, 476 (1991).
48. J. L. Holmes and M. Sirois, *Org. Mass Spectrom.* **25**, 481 (1990).
49. C. Wesdemiotis, A. Fura and F. W. McLafferty, *J. Am. Soc. Mass Spectrom.* **2**, 459 (1991).
50. *PROMATLAB Program*. MathWorks, Sherborn, MA, 1987.